

Enhanced Corrosion Resistance of Silicone-Modified Epoxy Coatings by Surface-Wave Plasma Treatment

Tao Xu^{1#}, Heqing Li^{2#}, Jing Song³, Guilian Wang¹, Seiji Samukawa⁴, Xijiang Chang^{1*}, Jingxia Yang^{2*}

¹ College of Electronic and Electric Engineering, Shanghai University of Engineering Science, 333 Long Teng Road, 201620, Shanghai, China

² College of Chemistry and Chemical Engineering, Shanghai University of Engineering Science, 333 Long Teng Road, 201620, Shanghai, China

³ Fashion & Art Design Institute, Donghua University, 1882 West Yanan Road, 200051, Shanghai, China

⁴ Advanced Institute for Materials Research, Institute of Fluid Science, Tohoku University, 2-1-1 Katahira, Aoba-ku, Sendai, 980-8577, Japan

T. Xu and H. Li contributed equally in this work.

* E-mail: 091031001@fudan.edu.cn (X. Chang); yjx09tj@foxmail.com (J. Yang)

Received: 4 February 2019 / Accepted: 13 March 2019 / Published: 10 May 2019

Silicone-modified epoxy coatings were prepared and treated under different plasma atmospheres in order to enhance their anticorrosion ability. The corrosion current density, corrosion potential and impedance of the modified coatings were measured by an electrochemical workstation. The results showed that the corrosion resistances of silicone-modified epoxy coatings were highly improved by surface-wave plasma treatment. Compared with the original coating, the corrosion current density of these coatings modified by plasma decreased from $0.5976 \mu\text{A}/\text{cm}^2$ to the minimum of $0.0058 \mu\text{A}/\text{cm}^2$ and the impedance increased from $1.925 \times 10^3 \Omega \cdot \text{cm}^2$ to the maximum of $2.938 \times 10^6 \Omega \cdot \text{cm}^2$, in which Ar plasma showed the best significant effect.

Keywords: silicone-modified epoxy, surface wave plasma, surface modification, corrosion resistance

1. INTRODUCTION

Epoxy resin is normally used as primer coating for anticorrosion because of its extreme adhesion to the substrate, but its thermal stability is limited and the anticorrosion ability normally needs to be improved, which can be achieved by addition of extra fillers/barriers [1-6] or modification the epoxy to improve the crosslinking of the resin [7]. In the second approach, silicone resin with high thermal stability was the most popular one, which can react with epoxy and form a silicone-modified epoxy coating to further improve the performance of the epoxy coating. This can take advantage of the

high thermal stability of the silicone resin and enhance the corrosion resistance of the epoxy resin by improving the crosslinking of the epoxy resin [8-14]. For example, Ahmad et al. synthesized an epoxy resin oligomer containing siloxane for plate printing by the addition reaction of ethylene sesquioxane and polydimethylsiloxane with one end sealed with ethyl epoxy cyclohexane structure. Afterwards, they find that the $T_{5\%}$ of the resin curing material was significantly increased up to 400 °C with the increase of the bridge base bond length [15].

However, chemical modification with silicone resin is not enough to improve the corrosion performance of the organic coatings because of the phase separation between silicone polymers and epoxy resins [16, 17]. A new surface-wave plasma technology can be used to effectively modify the surface of organic coatings to further enhance the corrosion resistance [18-21]. On the one hand, the plasma modification range of the coatings only involves the surface layer, but not the inside of the substrate, therefore, after plasma modification, the coating phase is not affected at all [22]. On the other hand, the plasma can effectively cover these micropores caused by the evaporation during the film formation to further prevent the intervention of corrosive media. Consequently, plasma has been applied to surface treatment of polymer coating and the surface properties were improved [18, 20]. For example, Li et al. used NH_3 plasma grafting epoxy coating process to modify the surface of aramid III, which increased the roughness of the fiber surface and improved its wettability [23]. Nevertheless, the influence of plasma treatment on silicone modified epoxy is still not very clear.

In this study, silicone oligomer was synthesized and further used to modify epoxy resin (E-51) by dealcoholization reaction between C-OH in epoxy resin and ethoxysilane-termination in organic silicone oligomer. The as-prepared silicone-modified epoxy coatings were treated with plasma to further enhance the corrosion resistance. The coating structures were examined by thermogravimetric analyzer (TGA), metallographic microscope and so on, and the anticorrosion abilities were evaluated by electrochemical test like potentiodynamic polarization curves and Nyquist plots by immersing the coating into 3.5 wt % NaCl solution. As expected, the plasma-treated coatings exhibited lower corrosion current densities. In order to explain the reason behind, the possible mechanism was proposed for the enhanced properties.

2. EXPERIMENTAL SECTION

Methyltriethoxysilane (MTES), dimethyldiethoxysilane (DMDES), phenyltriethoxysilane (PTES), xylene, tetrabutyl titanate, cyclohexanone and n-butanol were purchased from Aladdin Chemical Technology Co. Ltd. Shanghai (all were at least AR grade). Sodium bicarbonate, hydrochloric acid (HCl) and the curing agent (Amine 650) were bought from Sinopharm Chemical Reagent Co. Ltd.

2.1 Synthesis of silicone oligomer

Silicone oligomer was synthesized by modifying previous research [24]. MTES (17.83 g), DMDES (23.72 g), and PTES (24.04 g) were mixed with xylene (32.79 g) and added to a three-necked

bottle placed in a constant temperature oil bath set at 65 °C. The bottles were further mixed by a power agitator and then preheated for 10 min. The resulting mixed solutions were slowly dripped with deionized water (13.25 g) and the catalyst HCl (0.1 g) in a constant pressure burette. After 40 min of dripping, the oil bath temperature was immediately adjusted to 75 °C and the reaction solution was stirred at this temperature for 3 hours, thus forming the silicone oligomer.

After 3 h, additional NaHCO₃ (0.20 g) was added to the solution containing the newly generated silicone oligomer under further stirring to neutralize the HCl in the entire reaction system to pH=6~7. Then the stirring was stopped and the unreacted NaHCO₃ in the reaction system was removed by vacuum-filtering. Afterwards, the filtrate was collected. To make the reaction proceed in the direction of polymerization, the filtrate was further distilled under reduced pressure in a constant temperature oil bath at 80 °C. The distilled products contained a part of xylene and some low-boiling-point small-molecules substances such as ethanol and water. After the distillation rate was below a certain level and the products met the requirements, the products named the latest silicone oligomer in the three-neck bottle were collected.

2.2 Synthesis of silicone-modified epoxy coatings

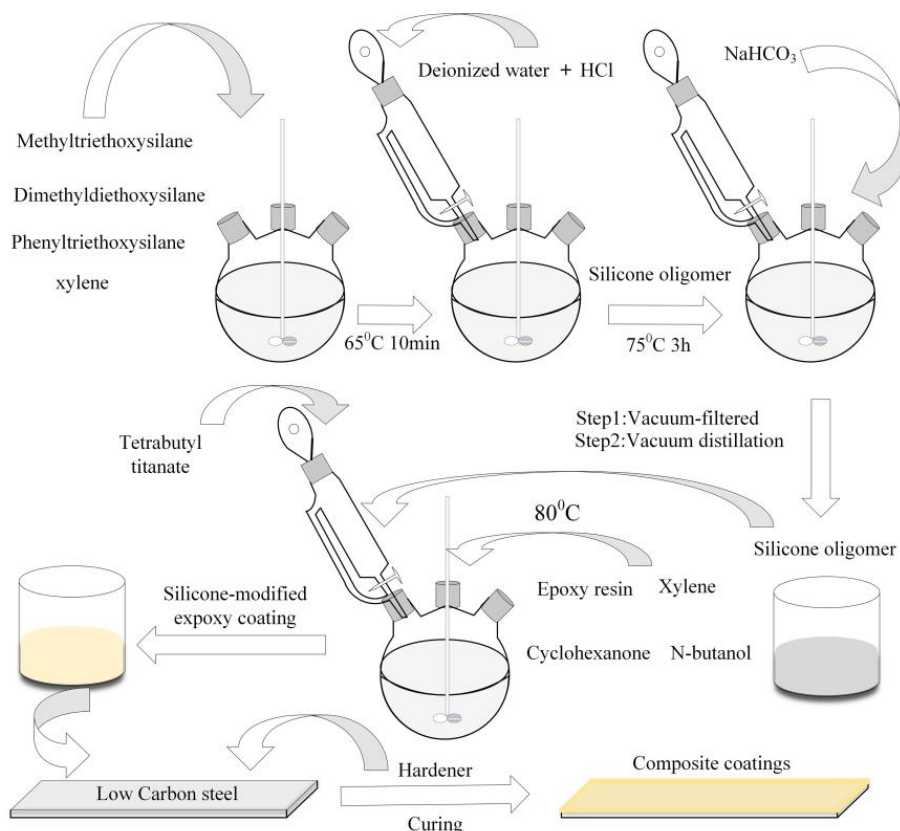


Figure 1. Illustration of the preparation procedure of the silicone-modified epoxy coating

Epoxy resin E51 (20.00 g) melted at 200 °C, xylene (28.00 g), cyclohexanone (4.00 g) and n-butanol (8.00 g) were mixed, stirred and then added to a three-necked bottle placed in a constant temperature oil bath at 80 °C for heat preservation. When the oil bath started to work, the mixed

solution containing the latest silicone oligomer (20.00 g /50 % solid) and tetrabutyl titanate (0.60 g) in the constant pressure burette were slowly added to the bottle. Under the stirring of the power agitator, the whole mixed solution in the bottle reacted completely. The reaction was stopped immediately after a sticky yellowish product appeared. In the end, the sticky yellowish product was diluted by xylene under stirring, forming a uniform silicone-modified epoxy coating.

The prepared silicone-modified epoxy coating was further coated on low carbon steel, which was sanded by sandpaper (#240), washed with alcohol repeatedly and then wiped dry before used. The silicone-modified epoxy coating was mixed with an equal quantity of curing agent under full stirring. Finally, a uniform and dense coating layer was formed by using a 100-nm-thick coating bar at room temperature on the substrate (150×50×2 mm). The production process flow of the silicone-modified epoxy coating was shown in Figure 1.

2.3 Plasma surface modification

The homemade surface-wave plasma generation equipment is shown in Figure 2. The microwave frequency is 2.45 GHz, and its power range is from 0.1 to 1 kW. The microwave power is coupled into the vacuum chamber via the slot antenna on the bottom side of rectangular waveguide. The quartz plate acts both vacuum sealer and boundary for the surface wave plasma excited. With the energy coupling adjusted by the three stub tuner and short plunger, the microwave power is transmitting into the processing chamber to breakdown the working gases, forming plasma on the bottom surface of the quartz plate. In this work, we tried plasma treatment with the following working gases: Ar, N₂, Ar+H₂ (1:1), Ar+NH₃ (1:1) and O₂. During plasma discharging, the pressure in the chamber was set around 20 Pa with the total gas flow rate of 50 sccm. The discharge power was set at 800 W with reflection power within 10 %. The sample was put on a stage with distance of 10 cm to the quartz plate and the plasma treatment time was 600 s for each sample.

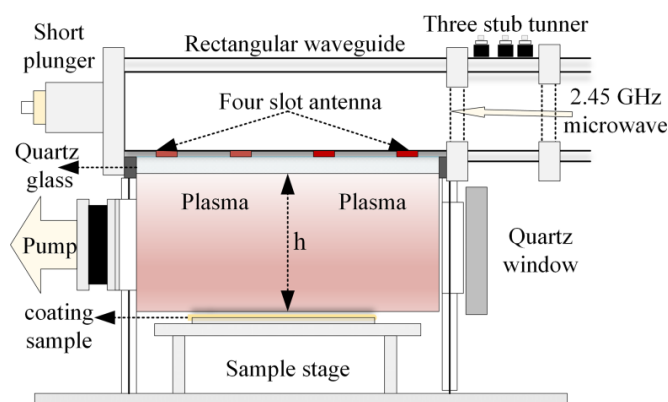


Figure 2. Schematic diagram of plasma generation equipment in this work

2.4 Characterization

The metallographic morphologies of the organic coatings were viewed by a polarizing microscope (BMM-580V, Batu, Shanghai). The coatings were also investigated on a Q500

Thermogravimetric analyzer (TGA) from 20 to 800 °C with ramping rate of 10 °C·min⁻¹ in air atmosphere (NETZSCH STA2500 from room temperature to 800 °C in air with 10 °C /min ramping rate). The hydrophilicity/hydrophobicity of the coatings was characterized by a contact angle meter (JC2000D2A, Zhongchen, Shanghai). Coating hardness, thickness and gloss were measured by pencil test, coating thickness gauge (Guangzhou Guouo Electronic Technology Co.) and an intelligent gloss meter (GB/T9966, Biaogeda, Guangzhou), respectively.

The organic coatings modified by plasma were immersed in a 3.5 wt % NaCl solution to characterize the electrochemical behavior [25-27]. Before the tests, three samples were immersed in the 3.5 wt % NaCl solution for 3 h, 6 days and 12 days, separately. Afterwards, the samples were detected by an electrochemical workstation with three electrodes. A saturated calomel electrode, a platinum sheet and coated electrode with an exposed surface area of 1 cm² were used as reference electrode, counter electrode and working electrode, respectively. The 3.5 wt % NaCl solution was used as the corrosive medium. Electrochemical impedance spectroscopy (EIS) was measured at different immersion time points over a frequency range of 100 k to 0.01 Hz, with alternating current amplitude of 0.005 V at open circuit potential. Finally, the EIS results were fitted on software of *Zsimpwin* [28-30].

3. RESULTS & DISCUSSION

3.1 Basic properties of coating

The silicone-modified epoxy coatings treated by different plasmas all had a consistent hardness rating of 3H (Table 1). The thickness of the (Ar+NH₃) plasma modified coating increased mainly because the amino functional group may be polymerized on the coating surface, forming a dense crosslinked layer [31]. The gloss of the plasma-modified coatings declined to different degrees compared with the original coating, which was a natural result of particles bombardment during plasma processing [32].

Table 1. Basic properties of the original coating and the coatings treated with different plasmas

Plasma	Hardness	Gloss(GU)	Thickness(μm)
Without plasma	3H	57.2	75.6
Ar plasma	3H	21.4	75.8
N ₂ plasma	3H	39.0	75.1
(Ar+H ₂) plasma	3H	23.0	77.4
(Ar+NH ₃) plasma	3H	22.9	83.4
O ₂ plasma	3H	21.0	76.0

Figure 3 shows the thermal stability of the as-prepared silicone-modified epoxy coatings before and after plasma treatment. TGA represents the quality loss of the coatings with increasing temperature. The derivative TGA (DTG) curves show the initial thermal decomposition temperature of these epoxy coatings is 350 °C and the complete decomposition temperature is about 470 °C. Plasma-

treated samples had less weight loss compared with the original sample, especially for the Ar plasma-treated sample. It can be explained by the cross-linking degree between silicone oligomer and epoxy resin. Higher cross-linking of silicone oligomer and epoxy resin indicated more OH groups condensed and more H₂O were formed and removed, resulting in less weight loss in TG test [33]. Thus the less weight loss of plasma-treated samples indicated that they had higher cross-linking degree than that of the untreated coating, and Ar was the best atmosphere among them. For NH₃ included plasma, there would be some cross linking layer formed with N radicals like NH₂-, NH-, etc. and carbon groups from plasma etching on the coating, which results slight weight gain [34].

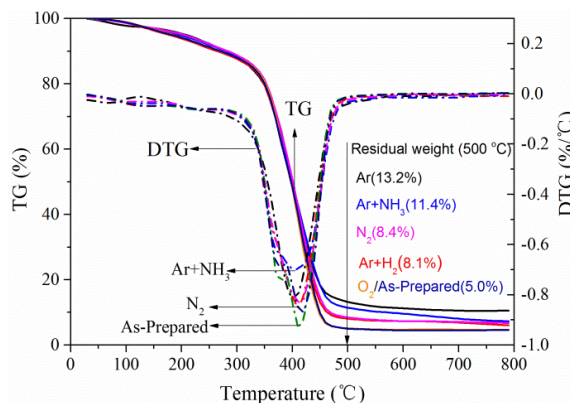


Figure 3. TGA curves of the silicone-modified epoxy coatings before and after plasma surface modification

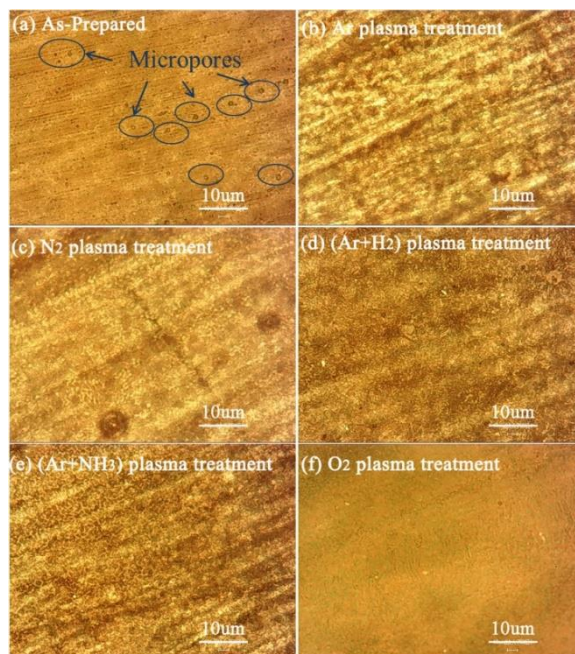


Figure 4. Metallographic images of surface of as-prepared silicone-modified epoxy coating (a) and plasma-treated coatings (b-f): (b) Ar plasma, (c) N₂ plasma, (d) (Ar+H₂) (1:1) plasma, (e) (Ar+NH₃) (1:1) plasma and (f) O₂ plasma, treatment times are all 10 min

Figure 4 shows the microscopic morphology of as-prepared silicone-modified epoxy coatings and plasma-treated coatings. From the Figure 4a we can find that there are many micropores on the surface of as-prepared silicone-modified epoxy coating, which were caused by the solvent evaporation during the coating was cured into a film on substrate at room temperature. The formed micropores on the coating cannot effectively block the corrosive medium (Figure 4a). In comparison, almost no micropores appeared on the surface of the plasma-treated coatings (Figure 4b-f), which was due to the effect of plasma modification [35]. The surfaces of the silicone-modified epoxy coatings treated by the latter three types of plasma were relatively rough and the one treated in the (Ar+NH₃)-plasma-is roughest among them (Table 1). Compared with other plasma treatments, the gloss of the O₂-plasma-modified epoxy coating was relatively low (Table 1). Meanwhile, the Ar-plasma-modified coating showed the best surface smoothness and best surface hydrophobicity [36].

The water permeability resistance and the protective properties of epoxy coatings are closely related [37]. Consequently, hydrophobicity does not allow the aqueous corrosion to stick on the coating surface, resulting in good anti-corrosive properties of these coatings. The contact angle was 84.3° in the as-prepared silicone-modified epoxy coating, and increased to 101.5° (Ar), 93.7° (N₂), 91.2° (Ar+H₂), 90.2° (Ar+NH₃) and 96.3° (O₂) for the coatings modified by five different plasmas, respectively (Figure 5). This suggested that the plasma treatment can increase the hydrophobic properties of the silicone-modified epoxy coatings. After heat-treatment at 200 °C, the water contact angles of the original, Ar-plasma-modified and N₂-plasma-modified coatings were 74.5°, 67.5° and 87.5°, respectively, which may be responsible for the worse corrosion resistance of these coatings after 200 °C heat-treatment.

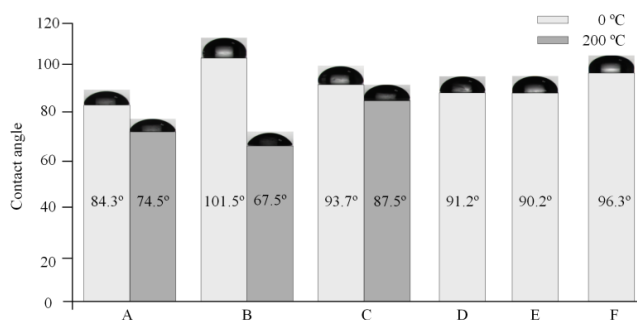


Figure 5. Contact angles of the as-prepared silicone-modified epoxy coating (A) and coatings treated with different plasmas (B-F): (B) Ar plasma, (C) N₂ plasma, (D) (Ar+H₂) (1:1) plasma, (E) (Ar+NH₃) (1:1) plasma, and (F) O₂ plasma. *Calcination at 200 °C for 10 min has been done with groups A, B and C as contrast

3.2 Electrochemical behavior of coatings

The polarization curves of the silicone-modified epoxy coatings were presented in Figure 6. The specific corrosion parameters of the coatings include corrosion current density (I_{corr}) and corrosion potential (E_{corr}) (Table 2). In general, the coating with a smaller corrosion current means that the coating possesses higher corrosion resistance [38]. Compared with the original silicone-modified

epoxy coating, the polarization curves of the plasma-modified coatings generally moved downward, indicating lower I_{corr} (Figure 6a). Specifically, the Ar plasma-modified coatings possessed the lowest I_{corr} , which might be associated with its smoother surface and higher cross-linking degree between silicone and epoxy resin.

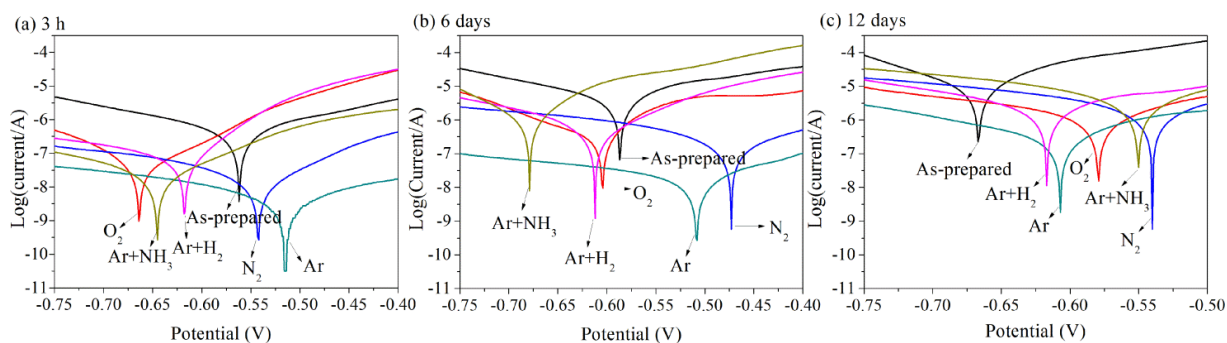


Figure 6. Tafel curves of the silicone-modified epoxy coatings with/without plasma treatment and further immersed in the 3.5 wt % NaCl solution for 3 h (a) , 6 days (b) and 12 days (c)

As the immersion time prolonging, the downtrend on the polarization curve of the N_2 plasma-modified epoxy coating was more pronounced compared with those of other plasma-modified samples, which implied that the N_2 -plasma-modified coating was more corrosion-resistant in NaCl solution. Meanwhile, the I_{corr} values of the Ar-plasma-modified coating were always the smallest compared with other parallel samples, no matter the immersion time was 3 h, 6 days, or 12 days, which were 0.0058 (3 h), 0.0247 (6 days), 0.3340 (12 days) $\mu\text{A}/\text{cm}^2$, respectively. Consequently, the silicone-modified epoxy coating treated in Ar plasma showed the best anticorrosion performance.

In addition, we investigated the temperature effects on the corrosion performance of the coatings (Figure 6a and Table 2). After 3 h of immersion in the 3.5 wt % NaCl solution, the corrosion current density (I_{corr}) of the original silicone-modified epoxy coating and the N_2 -plasma-modified coating calcined at 200 °C for 10 min increased a little. Surprisingly, the I_{corr} of Ar-plasma-modified coating varied greatly, which increased from 0.0058 to 9.5770 $\mu\text{A}/\text{cm}^2$. These results indicated that high temperature calcination reduced the corrosion resistance of plasma-treated silicone-modified epoxy coatings, as reported before [39].

Table 2. Electrochemical polarization parameters of the silicone-modified epoxy coatings with/without plasma surface modification after 3 h, 6 days, 12 days of immersion in the 3.5 wt % NaCl solution (pH=7)

Treatment methods	3 h		6 days		12 days		3 h (200°C)*	
	E_{corr} (V)	I_{corr} ($\mu\text{A}/\text{cm}^2$)	E_{corr} (V)	I_{corr} ($\mu\text{A}/\text{cm}^2$)	E_{corr} (V)	I_{corr} ($\mu\text{A}/\text{cm}^2$)	E_{corr} (V)	I_{corr} ($\mu\text{A}/\text{cm}^2$)
Primitive	-0.562	0.5976	-0.587	5.5140	-0.667	9.2110	-0.602	0.6282
Ar	-0.516	0.0058	-0.508	0.0247	-0.607	0.3340	-0.636	9.5770
N_2	-0.542	0.0173	-0.473	0.2801	-0.540	3.2060	-0.619	0.0190
$\text{Ar}+\text{H}_2$	-0.618	0.0705	-0.612	0.6041	-0.617	3.3270	----	----
$\text{Ar}+\text{NH}_3$	-0.645	0.0259	-0.679	0.9859	-0.550	5.5990	----	----
O_2	-0.664	0.0548	-0.604	0.2856	-0.579	1.7600	----	----

*Coatings calcined at 200 °C for 10 min.

Electrochemical impedance spectroscopies were tested to further verify the corrosion resistance of the silicone-modified epoxy coatings before and after plasma treatment. The Nyquist plots are shown in Figure 7. EIS is fitted by an electrochemical equivalent circuit as shown in Figure 8, where R_1 , R_2 , R_3 , CPE_{dl} and CPE_c are the solution resistance, coating resistance, charge transfer resistance, coating capacitance and double layer capacitance, respectively.

Moreover, a constant phase element (CPE) is used to facilitate the fitting. The impedance of the CPE is expressed as

$$Z_{CPE} = [f_0(j \times \omega)^n]^{-1}$$

Where f_0 is a proportionality coefficient, ω is the angular frequency and j is the imaginary unit. On account of the normal time constant distribution, the effective capacitance (Q) can also be calculated via the CPE parameters by:

$$Q = \frac{(Y_0 \times R)^{\frac{1}{n}}}{R}$$

where Y_0 and n are CPE admittance and CPE exponent, respectively [40].

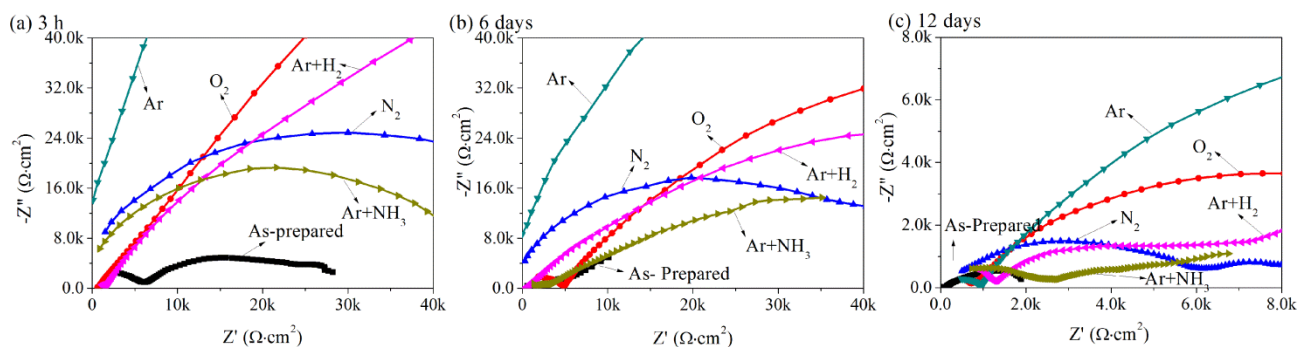


Figure 7. Nyquist diagrams of the silicone-modified epoxy coatings with/without plasma treated immersed in the 3.5 wt % NaCl solution for 3 h (a), 6 days (b) and 12 days (c) before and after plasma treatment

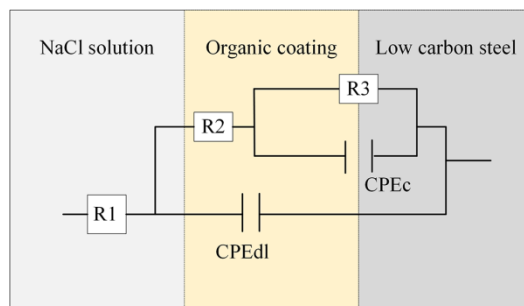


Figure 8. The equivalent electrical circuit used to fit the measured impedance data

It is generally accepted that the corrosion resistance of the coatings will be strengthened as the coating impedance increases [6]. As shown in Figure 7a, the diameter of the semicircles increases with the modification nearly in the rank of the Ar plasma > N₂ plasma > (Ar+NH₃) plasma > O₂ plasma > (Ar+H₂) plasma > the original. Therefore, after immersion in the 3.5 wt % NaCl solution for 3h, the

Ar-plasma-modified coating showed best anti-corrosion performance during all the electrochemical tests (Figure 7 a-c). Furthermore, the diameter of the N₂ and O₂ plasma-treated coatings were larger than the other types of plasma, which indicated the anti-corrosion properties of N₂ and O₂ plasma-modified coatings were slightly worse than the Ar-plasma one. The impedance fitting data were summarized in Table 3 for the plasma-modified coating immersed in the 3.5 wt % NaCl solution for 3 h, 6 days and 12 days. Previous research indicated that high R₃ represented a good anticorrosion ability, because R₃ suggested the resistance to aggressive species transfer [41, 42]. The as-prepared coating (3 h immersed in 3.5 wt % NaCl) showed R₃ of 2.742×10⁴ Ω. After plasma treatment, R₃ of the coating increased to 2.492×10⁵ Ω (Ar), 3.898×10⁵ Ω (N₂), 3.054×10⁵ Ω (Ar+H₂), 1.208×10⁶ Ω (Ar+NH₃) and 2.671×10⁵ Ω (O₂). This confirmed that the plasma-treated coating had better anticorrosion performance in NaCl solution.

Table 3 EIS fitting parameters of the silicone-modified epoxy coatings with/without plasma surface modification after 3 h, 6 days, 12 days of immersion in the 3.5 wt % NaCl solution (pH=7)

Treatment	R1 Ω·cm ²	Q-Yo F·cm ²	Q-n ---	R2 Ω·cm ²	Q-Yo F·cm ²	Q-n ---	R3 Ω·cm ²	
Prim	3h	4.331×10 ⁻⁴	7.159×10 ⁻¹⁰	0.955	1.925×10 ³	7.705×10 ⁻⁶	0.486	2.742×10 ⁴
	6day	1.358×10 ⁻⁵	1.059×10 ⁻⁶	0.531	8.952×10 ²	2.020×10 ⁻⁴	0.489	9.864×10 ³
	12day	4.387×10 ¹	1.175×10 ⁻⁵	0.662	7.563×10 ¹	6.224×10 ⁻⁴	0.539	2.220×10 ³
	3h(T ₂₀₀)	8.061×10 ¹	6.958×10 ⁻⁶	0.430	5.932×10 ²	1.027×10 ⁻⁶	0.727	2.448×10 ⁴
Ar	3h	2.401×10 ⁻⁷	1.942×10 ⁻⁹	0.812	2.938×10 ⁶	1.519×10 ⁻²³	0.650	2.492×10 ⁵
	6day	1.000×10 ⁻²	2.247×10 ⁻¹⁰	1.000	4.943×10 ⁴	7.962×10 ⁻⁸	0.434	6.562×10 ⁵
	12day	3.114×10 ⁻³	4.270×10 ⁻¹⁰	0.948	3.003×10 ⁴	1.499×10 ⁻⁶	0.437	1.072×10 ⁵
	3h(T ₂₀₀)	8.376×10 ¹	3.854×10 ⁻⁵	0.685	5.714×10 ³	3.596×10 ⁻⁴	0.810	7.111×10 ²
N ₂	3h	2.997×10 ⁻⁴	4.787×10 ⁻¹⁰	0.924	5.918×10 ⁴	2.549×10 ⁻⁷	0.655	3.898×10 ⁵
	6day	9.999×10 ⁻³	4.228×10 ⁻¹⁰	0.970	2.051×10 ⁴	1.329×10 ⁻⁶	0.522	1.631×10 ⁵
	12day	2.010×10 ¹	6.005×10 ⁻⁷	0.580	5.851×10 ³	1.473×10 ⁻⁴	0.435	3.912×10 ³
	3h(T ₂₀₀)	1.120×10 ⁻³	5.914×10 ⁻¹⁰	0.933	2.718×10 ⁴	8.331×10 ⁻⁶	0.344	9.745×10 ⁶
Ar + H ₂	3h	1.154×10 ⁻³	2.037×10 ⁻⁹	0.840	1.821×10 ⁴	1.205×10 ⁻⁷	0.793	3.054×10 ⁵
	6day	9.475×10 ²	2.271×10 ⁻⁵	0.427	8.312×10 ³	4.430×10 ⁻⁴	0.678	4.486×10 ⁴
	12day	1.004×10 ⁻²	1.505×10 ⁻⁸	0.744	1.796×10 ³	6.659×10 ⁻⁵	0.352	4.113×10 ⁵
Ar + NH ₃	3h	5.466×10 ⁻⁴	6.386×10 ⁻¹⁰	0.929	4.481×10 ⁴	1.761×10 ⁻⁶	0.624	1.208×10 ⁶
	6day	6.962×10 ⁻⁵	9.456×10 ⁻⁸	0.675	1.907×10 ³	2.424×10 ⁻⁴	0.233	1.137×10 ⁴
	12day	2.577×10 ⁻²	1.181×10 ⁻⁷	0.672	3.532×10 ²	3.238×10 ⁻⁵	0.614	8.306×10 ⁴
O ₂	3h	6.591×10 ²	5.459×10 ⁻⁷	0.764	2.564×10 ⁴	1.967×10 ⁻⁷	0.896	2.671×10 ⁵
	6day	6.880×10 ²	3.583×10 ⁻⁶	0.653	1.242×10 ⁴	1.181×10 ²	1.000	1.120×10 ¹²
	12day	1.258×10 ⁻⁸	5.865×10 ⁻⁹	0.808	6.619×10 ³	6.635×10 ⁻⁶	0.697	1.242×10 ⁵

The changes in impedance were also investigated before and after heat-treatment at 200 °C. According to the impedance spectroscopies (Figure 9b), the coating impedances were reduced obviously after the calcination at 200 °C and the anticorrosion ability of Ar-plasma-modified coating dropped mostly according to the impedance change. After calcined at 200 °C and being immersed in 3.5 wt % NaCl solution for 3 h (Table 3), R₃ of the as-prepared coating was 2.448×10⁴ Ω. But the value after Ar-plasma treated sample was only 7.111×10² Ω. Nevertheless, R₃ of N₂-plasma-treated sample sprisngly increased to 9.745×10⁶ Ω, confirmed that the N₂-plasma-treated coating still possessed better anticorrosion ability even after 200 °C calcination. Thus, the anti-corrosion

performance of coatings can be improved by plasma surface modification, especially the Ar-plasma at room temperature. But for high temperature application, N₂ would be the best plasma working gas.

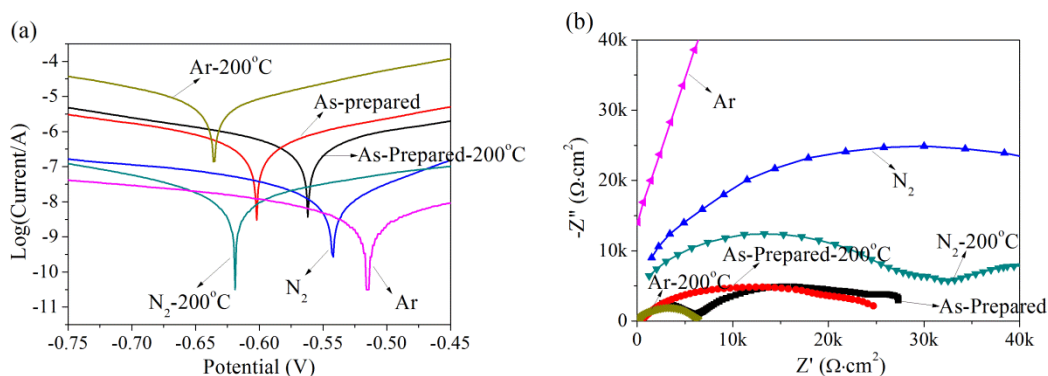


Figure 9. Tafel curves (a) and Nyquist diagrams (b) of the as-prepared silicone-modified epoxy coating and the coatings treated by Ar and N₂ plasmas after calcination at 200 °C and then immersed in the 3.5 wt % NaCl solution for 3 h

3.3 Anticorrosion mechanism

Base on the above results, the corrosion resistance of the silicone-modified epoxy coatings can be improved by plasma surface modification, especially for the Ar-plasma. Figure 10 showed the schematic diagram of anticorrosion mechanism after the plasma processing. During plasma processing, free radicals and particles reacted with OH, Si-OH groups on the coating surface, forming condensed layer via polymerization and crosslinking, which covered the micropores caused by the solvent evaporation during the film formation. This prevented the intervention of corrosive media (e.g. water molecules, oxygen and chloride ions) in the NaCl solution. Besides, random dispersion of plasma particles on the coating can generate a “labyrinth effect” to improve the barrier properties of the silicone-modified epoxy coating [43, 44], which can form a zigzagged the diffusion path and inhibit the penetration of the corrosive medium into the film.

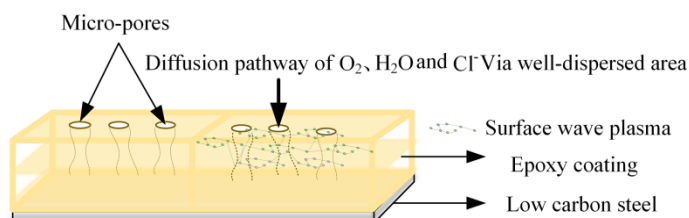


Figure 10. Corrosion resistance mechanisms of the plasma-modified coatings on metal substrate

4. CONCLUSIONS

Silicone-modified epoxy coatings were prepared and treated by plasma under different working atmospheres to enhance its anticorrosion properties. The films before and after plasma treatments were

examined by TGA, metallographic images, contact angle test, etc... The anticorrosion performances of the films were investigated through potentiodynamic polarization curves and EIS in 3.5 wt % NaCl solutions with different immersion time. According to the results of corrosion current density (I_{corr}), plasma treatment can effectively increase the coatings' corrosion resistance. The Ar-plasma-modified coating had the best anticorrosion performance at room temperature, which was mainly attributed to the smoother surface and higher hydrophobicity. After heat-treated at 200 °C, the corrosion currents of the original, Ar-plasma-modified and N₂-plasma-modified coatings were all increased, but the one by N₂-plasma-modification was the best one.

ACKNOWLEDGEMENT

This research is supported by National Natural Science Foundation of China (No. 21601121 and No. 11705115) and the Program for Professor of Special Appointment (Eastern Scholar) at Shanghai Institutions of Higher Learning (No. QD2016036 and No. QD2016037) and the Young Professor Cultivation Program of Shanghai Municipal University (No. ZZGCD16006 and No. ZZGCD16019). This work is also sponsored by Shanghai Pujiang Program (No. 18PJC002) and SUES Innovation Project for Graduate Students (18KY0405). Part of the work was carried out under the Collaborative Research Project of the Institute of Fluid Science, Tohoku University.

References

1. S. Gonzalez, M.A. Gil, J.O. Hernandez, V. Fox and R.M. Souto, *Prog. Org. Coat.*, 41 (2001) 167.
2. D. Ramesh and T. Vasudevan, *Prog. Org. Coat.*, 66 (2009) 93.
3. H. Wang, F. Presuel and R.G. Kelly, *Electrochim. Acta*, 49 (2004) 239.
4. Y. Zhu, J. Xiong, Y. Tang and Y. Zuo, *Prog. Org. Coat.*, 69 (2010) 7.
5. D. Yu, S. Wen, J. Yang, J. Wang, Y. Chen, J. Luo and Y. Wu, *Surf. Coat. Technol.*, 326 (2017) 207.
6. L. Guo, L. Jing, Y. Liu, B. Zou, S. Hua, J. Zhang, D. Yu, S. Wang, L. Wang and J. Yang, *Int. J. Electrochem. Sci.*, 13 (2018) 11867.
7. M. Liu, X. Mao, H. Zhu, A. Lin and D. Wang, *Corros. Sci.*, 75 (2013) 106.
8. S. Ananda Kumar and T.S.N. Sankara Narayanan, *Prog. Org. Coat.*, 45 (2002) 323.
9. S. Ammar, K. Ramesh, B. Vengadaesvaran, S. Ramesh and A.K. Arof, *Prog. Org. Coat.*, 92 (2016) 54.
10. Z. Heng, Z. Zeng, Y. Chen, H. Zou and M. Liang, *J. Polym. Res.*, 22 (2015) 1.
11. R. Li, C. Zhou, Y. Chen, H. Zou, M. Liang and Y. Li, *High Perform. Polym.*, 29 (2017) 36.
12. Q. Ren, H. Zou and M. Liang, *J. Appl. Polym. Sci.*, 131 (2014) 40212/1.
13. R. Wen, J. Huo, J. Lv, Z. Liu and Y. Yu, *J. Mater. Sci.: Mater. Electron.*, 28 (2017) 14522.
14. L.J. Matienzo and F.D. Egitto, *J. Mater. Sci.*, 41 (2006) 6374.
15. M.R. Ramli, R. Ramli, K. Mohamed and Z. Ahmad, *Macromol. Mater. Eng.*, 303 (2018) n/a.
16. S. Li, H. Li, Z. Li, H. Zhou, Y. Guo, F. Chen and T. Zhao, *Polymer*, 120 (2017) 217.
17. S. Li, F. Chen, B. Zhang, Z. Luo, H. Li and T. Zhao, *Polym. Degrad. Stab.*, 133 (2016) 321.
18. J.N. Borges, T. Belmonte, J. Guillot, D. Duday, M. Moreno-Couranjou, P. Choquet and H.-N. Migeon, *Plasma Processes Polym.*, 6 (2009) S490.
19. J.F. Coulon, N. Tournier and H. Maillard, *Appl. Surf. Sci.*, 283 (2013) 843.
20. X. Jin, W. Wang, C. Xiao, T. Lin, L. Bian and P. Hauser, *Compos. Sci. Technol.*, 128 (2016) 169.
21. N. Mukherjee, D. Wavhal and R.B. Timmons, *ACS Appl. Mater. Interfaces*, 2 (2010) 397.
22. M. Chaker, M. Moisan and Z. Zakrzewski, *Plasma Chem. Plasma Process.*, 6 (1986) 79.
23. S. Li, X.-z. Li, H.-j. Kong, K.-q. Han and M.-h. Yu, *Hecheng Xianwei*, 43 (2014) 26.
24. A. Zhang, C. Chang and y. Jia, *Applied Mechanics and Material*, 713-715 (2015) 2644.

25. N.W. Khun, E. Liu and X.T. Zeng, *Corros. Sci.*, 51 (2009) 2158.
26. J. Liang, P.B. Srinivasan, C. Blawert and W. Dietzel, *Corros. Sci.*, 51 (2009) 2483.
27. O. ur Rahman and S. Ahmad, *RSC Adv.*, 4 (2014) 14936.
28. E. Akbarinezhad and H.R. Faridi, *Surf. Eng.*, 24 (2008) 280.
29. M. Mahdavian, M.M. Attar, *Corros. Sci.*, 48 (2006) 4152.
30. M. Mahdavian, M.M. Attar, *Electrochim. Acta*, 50 (2005) 4645.
31. H.-L. Lu, L. Sun, S.-J. Ding, M. Xu, D.W. Zhang and L.-K. Wang, *Appl. Phys. Lett.*, 89 (2006) 152910/1.
32. F.M. Donahue and K. Nobe, *J. Electrochem. Soc.*, 112 (1965) 886.
33. W.-D. He, Y.-F. Zou and C.-Y. Pan, *J. Appl. Polym. Sci.*, 69 (1998) 619.
34. H. Nagai, M. Hiramatsu, M. Hori and T. Goto, *J. Appl. Phys.*, 94 (2003) 1362.
35. M.S. Kang, B. Chun and S.S. Kim, *J. Appl. Polym. Sci.*, 81 (2001) 1555.
36. P. Samyn, G. Schoukens, H. Van den Abbeele, L. Vonck and D. Stanssens, *J. Coat. Technol. Res.*, 8 (2011) 363.
37. B. del Amo, L. Veleva, A.R. Di Sarli and C.I. Elsner, *Prog. Org. Coat.*, 50 (2004) 179.
38. G. Ruhi, H. Bhandari and S.K. Dhawan, *Prog. Org. Coat.*, 77 (2014) 1484.
39. X. Liu, Y. Shao, Y. Zhang, G. Meng, T. Zhang and F. Wang, *Corros. Sci.*, 90 (2015) 463.
40. J.-B. Jorcin, M.E. Orazem, N. Pebere and B. Tribollet, *Electrochim. Acta*, 51 (2006) 1473.
41. J. Fu, T. Chen, M. Wang, N. Yang, S. Li, Y. Wang and X. Liu, *ACS Nano*, 7 (2013) 11397.
42. M. Wang, M. Liu and J. Fu, *J. Mater. Chem. A*, 3 (2015) 6423.
43. A.H. Navarchian, M. Joulazadeh and F. Karimi, *Prog. Org. Coat.*, 77 (2014) 347.
44. E. Potvin, L. Brossard and G. Larochelle, *Prog. Org. Coat.*, 31 (1997) 363.

© 2019 The Authors. Published by ESG (www.electrochemsci.org). This article is an open access article distributed under the terms and conditions of the Creative Commons Attribution license (<http://creativecommons.org/licenses/by/4.0/>).